15

Zappa, a Compliant Quasi-Passive Biped Robot with a Tail and Elastic Knees

Félix Monasterio-Huelin and Álvaro Gutiérrez
Universidad Politécnica de Madrid
Spain

Fernando J. Berenguer
Fundación Prodintec
Spain

1. Introduction

Bipeds are complex hybrid dynamical systems mixing both continuous and discrete-event phenomena (Hurmuzlu et al., 2004). The main characteristic of biped walkers is the abrupt kinematic change between the swing phase and the stance phase together with dynamical impacts. The main problem is how to achieve a rhythmical or periodical walk. Another difficulty of these robots is their high power requirement and, consequently, high energy consumption, which limits their autonomy. It can be attributed to the high number of actuated joints, and because energetic studies are not typically considered during the movement's planning.

Different studies focusing on the construction of locomotion controllers for completely actuated legged robots are found in the literature. These studies are mainly oriented to solve trajectory generation problems for the active control centered approach. In (Boeing & Bräunl, 2004) the authors show there is an example of this methodology showing that an impedance control is better than the computed torque method. However, the conventional approach has been questioned by researchers inspired by biomechanical models (Kuo, 2007; McMahon, 1984). The discovery of McGeer about passive dynamic walking by building a biped without any motors or sensors (McGeer, 1990), opens the doors to a new design concept based on morphological considerations. Moreover, the interaction between morphology and control is a topic of actual researches and debates in robotics (Pfeifer & Bongard, 2007). Therefore, exploiting the intrinsic passive dynamics has many advantages compared to the classical two-part methodology (trajectory generation and active controller). Two of them are the energy consumption reduction (the energetic cost is produced in step-to-step transitions) and the simplicity of control (low computational cost). Nevertheless, some theoretical and practical studies (Collins & Ruina, 2005) show that it is difficult to achieve the complex dynamics exhibited by humans and animals taking into account only the properties of simple passive-dynamic walking, but might help in the design of walking robots. In (Fumiya & Pfeifer, 2006) the authors show how to exploit the above mentioned passive properties of biped robots with the incorporation of sensors.

Typically, bipedal walking models assume rigid body structures. On the other hand, elastic materials seem to play an essential role in nature (Alexander, 2005). Therefore, spring-damper elements have been proposed as an initial solution for the compliant leg concept (Fumiya et al., 2009; Geyer & Seyfarth, 2006). These solutions can be extended with adaptable compliance (inverse of stiffness) mechanisms (Ham et al., 2007).

A mechanism for a real biped robot with a tail (i.e. *Zappa*) was proposed in (Berenguer & Monasterio-Huelin, 2006) and improved in (Berenguer & Monasterio-Huelin, 2008). *Zappa* is a robot able to walk in flat floors of different positive and negative slopes (Gutiérrez et al., 2008). The tail is the only actuated limb that imposes an oscillatory movement of variable frequency. By using this simple idea, it is possible to achieve an inverted pendulum trajectory for the legs. In this work, we propose a structural modification to *Zappa*, by adding elastic knees to the robot. This solution offers two main advantages: *(i)* a greater maneuverability and *(ii)* more compliant gaits.

The paper is organized as follows. In Section 2 the robot kinematics are fully described. In section 3 we propose a new controller applied to the robot's tail. Moreover, we study the robot energy consumption, and focus on the robot initialization, as a restriction to the walking performance. Section 4 describes the robot parameters along with performance graphs. Finally, Section 5 summarizes the most relevant conclusions and suggests future research directions.

2. The mechanism of the biped robot and the gait pattern

2.1 Kinematic Description

The previous implementation of *Zappa* (see Figure 1) had two legs, each composed of a four bars mechanism, four hip bars and a tail. The four bar mechanism includes a two bars femur, a one-bar foot and one hip's bar. The hip is composed of four bars, two of them joining the two bars femur of each leg, and the others two joining the legs. The tail is attached to one bar of the hip. The frontal plane is the ZY plane, the sagittal one is the XY plane and the transverse one is the ZX. To talk about the mechanism, we describe the following nomenclature as an example: A represents the line of the ankles, and AL and AR the left and right A lines respectively. When needed we will write AFL and ABL for the front and back of AL bars respectively. Figures 2a, 2b and 3a show the disposition of all bars and rotational joints. The foot has four possible contact points (C) with the floor (or ground, G) as depicted in Figure 3b. To start walking, it is enough to move the tail around the Y axis and to fix a spring to the ABL and ABR ankles. In Zappa this movement is managed by a DC servomotor with a position sensor controlling the tail and an extensional spring holding the back femur and the foot. Nevertheless, in simulations we use a torsional spring for the ankles and a controller to generate torque for the tail joint, as explained in Section 2.2.

The superior bar in the hip is added to avoid independent rotations of the legs around the X axis (see Figure 4). This bar is redundant in the stance phase. In general, this bar fixes a kinematic constraint to the hip angle:

$$q_{1R} - q_{1L} = \pi \tag{1}$$

This constraint could be relaxed adding a extensional spring ($q_5 = x_5$). The advantage of relaxing this constraint is to gain maneuverability to facilitate the rotation of the biped around the Y axis, and to avoid the sliding of the feet in the stance phase. In this work, we do not study the different configurations. On the other hand, the spring has been adjusted to generate enough force to avoid this balancing.

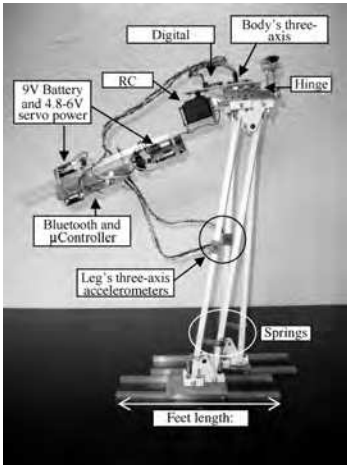
Digital
Body's three-axis
RC
Hinge
9V Battery and 4.8-6V servo power
Bluetooth and µController
Leg's three-axis accelerometers
Springs
Feet length:

Fig. 1. Zappa biped robot. Prototype without knees.

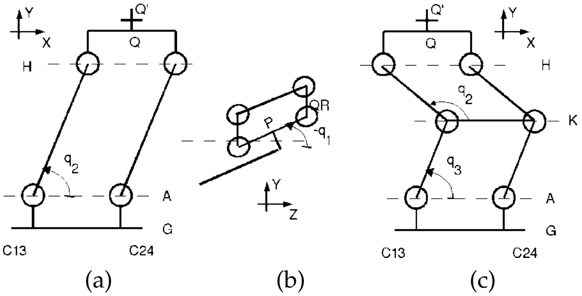
Y
X
Q'
Q
H
q2
A
G
C13
C24
R
P
-q1
Y
Z
Q'
Q
Y
X
H
q2
K
q3
A
G
C13
C24

(a) (b) (c)

Fig. 2. Sagittal plane of a leg (a) without and (c) with knee. (b) Frontal plane of the hip bars and the tail.

For the stance phase there is a strong kinematic constraint that is avoided by producing a slight sliding of the feet in the Z direction, as depicted in Figure 5,

$$l_2 sin(q_{2R}) + l_1 sin(q_1) = l_2 sin(q_{2L}) \tag{2}$$

In the particular situation of $q_1 = 0$, the sole solution is $q_{2R} + q_{2L} = \pi$ or $q_{2R} = q_{2L}$. Therefore, the center of the hip bars will always lie in the midpoint between the feet. Furthermore, the distance between the feet depends on one ankle angle: $L = 2lcos(q_2)$.

To avoid the sliding, we propose to relax the latter kinematic constraint adding a knee. To do this, we have divided the femur in two parts, from now on femur and tibia, as depicted in Figure 2c (q_2). If the knee bar is rigid, each leg femur bars are parallel, and so are the tibia bars. The second kinematic constraint has been broken, but the pentagonal kinematic closed chain imposes a new constraint:

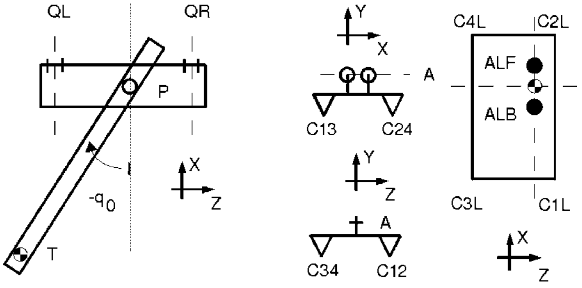
QL
QR
P
-q0
T
X
Z
Y
X
A
C13
C24
Y
Z
A
C34
C12
C4L
C2L
ALF
ALB
C3L
C1L
X
Z

(a) (b)

Fig. 3. (a) Transverse plane of the Central Hip and the Tail. (b) Three planes of a foot: joints with the leg and contact points with the floor.

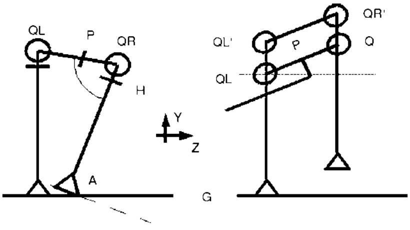
QL
P
QR
H
A
Y
Z
G
QR'
QL'
P
Q
QL

(a) (b)

Fig. 4. Hip superior bar added to avoid oscillations around the X axis.

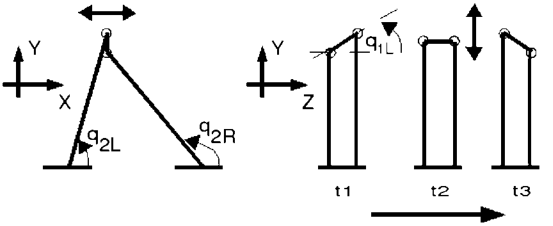
Y
X
q2L
q2R
Y
Z
q1L
t1
t2
t3

(a) (b)

Fig. 5. (a) A possible configuration during the stance phase. (b) A possible time sequence t_1-t_3 to show the needed feet sliding in Z direction for the robot without knees.

$$l_3 sin(q_{3R}) + l_2 sin(q_{2R}) = l_3 sin(q_{3L}) + l_2 sin(q_{2L}) \tag{3}$$

As shown in Figure 6, a robot with knees is able to move from posture I to posture II without modifying the distance L and without sliding. Moreover, we observe point O changes its relative position and the height of the hip to the ground also varies. Therefore, this way of moving is more compliant.

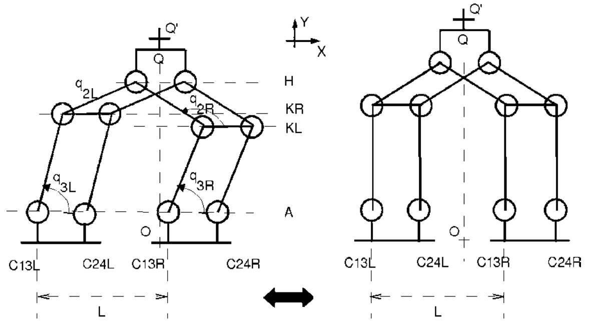

(I) (II)

Fig. 6. A possible movement of the robot with knees which avoids the sliding in the Z axis.

Both in the swing and the stance phase the feet are parallel to each other, both in the biped with and without knees. However, if we add elastic knees to the robot, we are able to avoid this third kinematic constraint, obtaining interesting properties. For example, with the feet completely aligned the sole solution is the one shown in Figure 7a. With only one foot on the floor it is possible that the other leg is in the posture of Figure 7b. This mechanism adds two new degrees of freedom (dof) to the robot (q_4) (one translational dof for each leg).

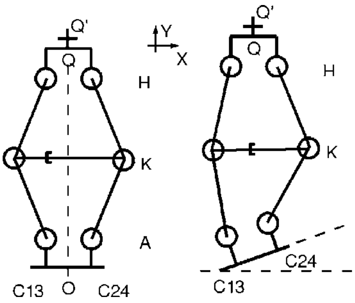

(a) (b)

Fig. 7. Two possible postures for the robot with elastic knees.

2.2 Gait Description

As shown in Figure 2c, the springs are rotational in the ankles (ABL, ABR, q_3) and in the knee/femur (joining the femur and the knee bar; KBL, KBR, q_2). In the knee bar (line K, $q_4 = x_4$) and in the superior hip bar (line Q′, $q_5 = x_5$) the springs are extensional. They are modelled as linear torque or force generators according to the equations:

$$\tau_i = -k_i(q_i - q_i^0) - b_i\dot{q}_i, \quad i = 2,3 \tag{4}$$

$$F_i = -k_i(x_i - x_i^0) - b_i\dot{x}_i, \quad i = 4,5 \tag{5}$$

where q_i^0 and x_i^0 are the i-spring equilibrium position, k_i the i-spring constant and b_i the i-viscous damping coefficient.

Selecting the springs is far from a trivial task as shown in (Gutiérrez et al., 2008). In that work, the authors studied a variable tuning for the ankle spring in the biped without knees using evolutionary optimization techniques. The fitness function was the travelled distance in a specified time and at different slopes of the floor. A mechanism that is able to change the spring parameters in real time was proposed in (Ham et al., 2007) using two servomotors (in general it is possible to generate the spring torque or force with only one DC motor and an electrical current controller). In the present work we have empirically obtained constant parameters by means of computer simulations.

One important question, not mentioned before, is related to the reaction forces between the feet and the ground. This question is extremely important in walking robots because of the strokes that occur when changing from the swing phase to the stance phase, and because they are variables that show the biped stability.

The total reaction force ($\mathbf{F}_R$) of the robot satisfies the following vectorial equation,

$$\mathbf{F}_R = M(\ddot{\mathbf{cm}} - \mathbf{g}) \tag{6}$$

where $\ddot{\mathbf{cm}}$ is the acceleration of its center of mass referred to some inertial coordinates system, $\mathbf{g}$ the gravitational acceleration and M the mass of the robot. The Newton equation of a foot is

$$\mathbf{f}_R + \mathbf{f}_{AB} + \mathbf{f}_{AF} + m_F\mathbf{g} = m_F\mathbf{a}_F \tag{7}$$

where $\mathbf{f}_R$ is the reaction force of one leg, m_F the mass of the foot, $\mathbf{f}_{AB}$ and $\mathbf{f}_{AF}$ the forces exerted by the back femur (or tibias, for the robot with knees) and frontal femur respectively on the foot (ankles AB and AF).

Hence, $\mathbf{F}_R = \mathbf{f}_{RL} + \mathbf{f}_{RR}$. When the foot is on the floor $\mathbf{a}_F = \mathbf{0}$. In the other case $\mathbf{f}_R = \mathbf{0}$. Therefore, measuring $\mathbf{a}_F$ is enough to know if one leg is on the floor except in the case of elastic knees, because the foot may oscillate around the Z axis. Simulations made in this work consider that the foot is in the air if all the reaction forces at each contact point in the three directions of space (x,y,z) are zero. Figure 8 shows the timing of the moments of contact of feet with the ground (represented as zero) overlapped with the reaction forces of each foot.

For the computer simulations, we have modelled the contact point between the feet and the floor as attractive forces that depend on the velocity of each foot contact point for the X and Z direction. For the Y direction, a stiffness factor has been added. This factor depends on the position only when position and velocity are negative (Berenguer & Monasterio-Huelin, 2007a).

Most figures that follow have been overlapped with this timing to properly interpret them.

The functioning of the biped robot is as follows: when $q_0 = 0$ the robot remains standing. For $\mu(t)$ around $\pi/2$ the robot rises a leg while the other remains in the floor. In other words, the tail works as a dynamic counterweight varying q_1. Because of the torque applied to the tail joint, the moment produced in the legs creates a pendular oscillation in both legs. This oscillation is produced around the ankle (A) for the foot on the floor and around the hip (H) for the foot in the air. This oscillation depends on all the springs of the robot. The potential energy stored in the springs acts as an energy generator allowing a compliant walking.

To be more concise, we can distinguish a clear sequence of movements of point P (tail joint) during the turn of the tail. The swing phase begin lifting one leg when $q_0 = \pi/2 - \mu$ until $\pi/2$, and provokes that $\dot{P}_x > 0$. From $\pi/2$ until $q_0 = \pi/2 - \mu'$ the swing phase continues until the foot makes contact with the ground; hence $\dot{P}_x > 0$. In the stance phase $\dot{P}_x$ changes

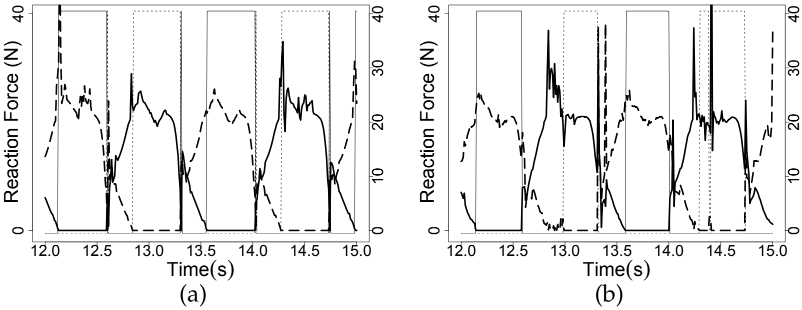

Fig. 8. Left (solid) and Right (dashed) feet reaction forces for a robot (a) without knees and (b) with elastic knees.

its sign until $q_0 = -\pi/2 + \mu$, repeating the cycle. Figure 9 shows this sequence. In Figure 10 the limit cycle ($\dot{q}_2$ versus q_2 for the robot without knees, $\dot{q}_3$ versus q_3 and $\dot{q}_2$ versus q_2 for the robot with elastic knees) of the biped gait pattern is shown. We define the limit cycle as a sequence of steps used as an index of whole stability (Hobbelen & Wisse, 2007) in contrast to the ZMP (Vukobratovic et al., 1990) that imposes local stability at every instant in time.

In Figure 9 we show the P_y kinematic equation when all the four contact points of the foot are in the floor. However, this is not the general case when the robot has elastic knees because P_y depends on the angle between the foot and the floor in the stance phase. Therefore, the biped robot with elastic knees walks raising the heel (line C13 in Figure 3b) of the swinging leg and falls on it at the end of a step (in a similar way to human walking).

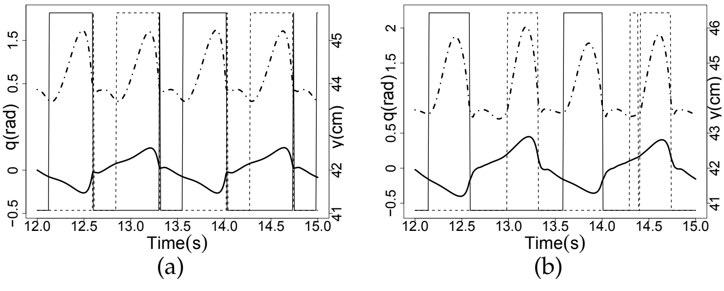

Fig. 9. q_{1L} (solid) and P_y (dotdashed) of the biped (a) without knees (in the stance phase $P_{yL} = l_1\,|sin(q_{1L})| + l_2 sin(q_{2L})$) and (b) with elastic knees (in the stance phase $P_{yL} = l_1\,|sin(q_{1L})| + l_2 sin(q_{2L}) + l_3 sin(q_{3L})$ with no elastic knees, as explained in the text).

The angular position and torque of the Knee/Femur spring and the linear position and force of the Knee spring are shown in Figure 11.

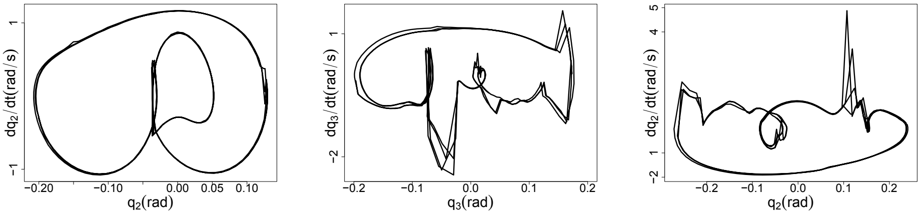

(a) (b) (c)

Fig. 10. Limit cycle of the biped (a) without knees. (b) $\dot{q}_3$ versus q_3 and (c) $\dot{q}_2$ versus q_2 with elastic knees.

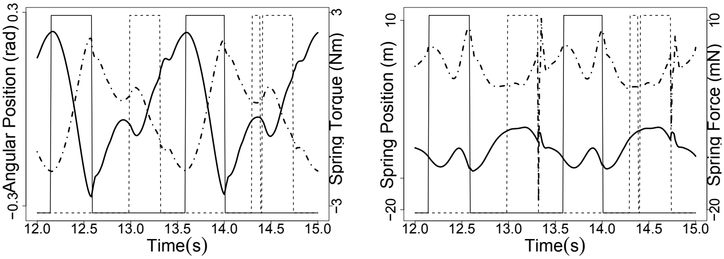

(a) (b)

Fig. 11. (a) Left (dotdashed) and Right (solid) femurs torques of a robot with elastic knees. (b) Left (dotdashed) and Right (solid) knees forces of a robot with elastic knees.

3. Tail control, power consumption and stability of the biped

To achieve a regular walking gait the tail has to be controlled adequately. This can be done imposing a sinusoidal movement to the tail (q_{0r}). However, because all initial conditions are zero (the robot is with both feet together) and because an abrupt change could make the biped to fall, a special starting procedure is needed. The idea is to begin the walk with short strides before imposing a sinusoidal oscillation of constant frequency f. In (Berenguer & Monasterio-Huelin, 2007b) chirp functions were used to study the dependency of this starting procedure as a function of frequency variation. In this work, we use a chirp function to switch to the sinusoidal by imposing continuity conditions in position, velocity and acceleration. For these reasons, there is only one solution depending on two parameters: (i) the time at which the switch occurs (t_f) and (ii) the number of periods the chirp must perform (N).

$$q_{0r} = \begin{cases} \pi/2sin(at^2), & t < t_f \\ \pi/2sin(2\pi f(t-t_f) + (2N-1)\pi/2), & t \geq t_f \end{cases} \tag{8}$$

where $a = (2N-1)\pi/(2t_f^2)$. Figure 12 shows the reference signal for the tail.

To control the tail, we set up this chirp function as the reference signal. The tail satisfies the following two vectorial Newton-Euler equations:

$$\mathbf{f}_T + m_T\mathbf{g} = m_T\mathbf{a}_T \tag{9}$$

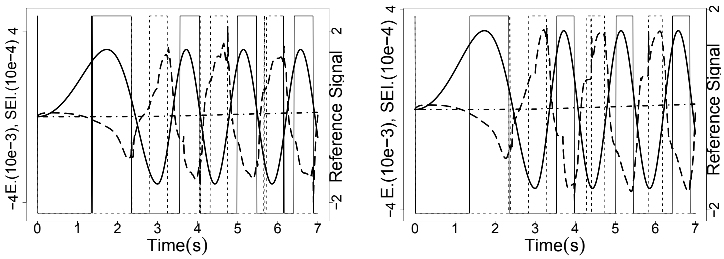

(a) (b)

Fig. 12. Reference signal (solid) (q_{0r}) with $t_f = 3s$, $N = 2$, error signal (dashed) and squared error integral (dotdashed) for a PD with $k_p = 300$ and $k_D = 20$. (a) Without knees and (b) with elastic knees.

$$\boldsymbol{\tau}_T + \mathbf{f}_T x \mathbf{l}_0 = \mathbf{I}\boldsymbol{\alpha} + \boldsymbol{\omega}\, x(I\boldsymbol{\omega}) \tag{10}$$

where $\mathbf{a}_T$ is the linear acceleration of the tail center of mass, m_T the mass of the tail, $\mathbf{g}$ the gravitational acceleration, $\mathbf{l}_0$ the radial vector from the tail joint to the tail center of mass, $\mathbf{I}$ the tail inertia matrix, $\boldsymbol{\alpha}$ the tail angular acceleration, and $\boldsymbol{\omega}$ the tail angular velocity.
Solving these equations in the Y direction (tail's rotation axis) and assuming a punctual mass, we obtain the mechanical torque that must be applied to the tail:

$$\tau_T = m_T l_0 a_{Tz'} \tag{11}$$

where z' is the Z component in the frame attached to the tail.
The linear acceleration of the tail center of mass (when no sliding) in the stance phase is

$$a_{Tz'} = l_0 \ddot{q}_0 + \ddot{P}_{z'} \tag{12}$$

where $\ddot{P}_{z'}$ is the linear acceleration of point P in the frame attached to the tail joint with respect to the inertial coordinate system projected in the z' axis.
In the stance phase and assuming there is not sliding, the tail joint has no Z component, and the X and Y components are because of the pendular movement of the legs around the ankles. As aforementioned, the biped without knees cannot avoid this sliding (see Figure 5) but it is kinematically possible for a biped with knees to do it.
The controller we propose applies a torque to the tail joint following Equation 13 (a feedforward term and a PD feedback controller):

$$\tau_T = m_T l_0 a_{Tr} + k_P e + k_D \dot{e} \tag{13}$$

where $e = q_{0r} - q_0$, $a_{Tr} = l_0 \ddot{q}_{0r}$, and k_P and k_D constants that must be tuned.
Taking into account the mechanical torque and ordering the terms we obtain the Laplace error equation,

$$(m_T l_0^2 s^2 + k_D s + k_P)E(s) = m_T l_0 \mathcal{L}(\ddot{P}) \tag{14}$$

If we select stable poles and $\lim_{s \to 0} s\mathcal{L}(\ddot{P}) = 0$, the steady-state error will be zero. The transient response will be very short when choosing the poles with high values. Figure 12 shows the error signal and the squared error integral.

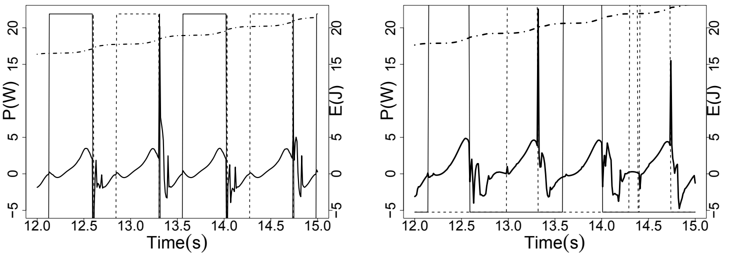

(a) (b)

Fig. 13. Energy (dotdashed) and Power consumption (solid) for a robot (a) without knees and (b) with elastic knees in the time interval from 12 to 15 seconds.

Another important problem for biped robots is the mechanical power ($P(t)$) and energy ($E(t)$) consumption. Because the tail is the only actuated joint, we can define them using the following relations:

$$P(t) = \tau_{Tz}\dot{q}_0 \tag{15}$$

$$E = \int_0^t |P(t)|\, dt \tag{16}$$

Figure 13 shows the power and energy consumption.

As mentioned in Section 2.2 the limit cycle shown in Figure 10 could be used to analyze the cyclic stability of the biped. This study would proceed gait by gait searching a stable periodic motion, although it might not be a stable motion in every instant of time. In this work we do not analyze this important question, and we do not know if the system is stable in either one sense (cyclically) or the other (locally). Actually, we know that the robot with elastic knees does not fall and we consider it as a proof of its stability. This analysis remains to be done in a near future.

4. Simulation Studies

The robot has been simulated thanks to the *SimMechanics* toolbox included in the *Matlab* software. Robots with and without knees maintain the same weight. The femur and the tibia have been blocked in the robot with knees to simulate the robot without knees. The task performs a straight line walking for 15 simulated seconds where the tail's frequency oscillation is 0.7 Hz for both simulated robots.

The main parameters of the robot used in simulations are presented in Table 1 where the "K" corresponds to the robot with knees. (Note that $l_2 = l_{2K} + l_{3K}$). The constant "d" represents the distance between frontal and back bars of a leg.

Finally, the different values of the springs parameters are presented in Table 2.

5. Conclusions and future work

Comparing a biped with and without knees is a hard problem because of their structural differences. Nevertheless, in this work we have stated there are at least two measurements that

Name	Value	Name	Value	Name	Value
m_{tail}	760 gr.	l_0	150 mm.	d	40 mm.
m_{hip}	210 gr.	l_1	100 mm.	$lfoot_{C12}$	320 mm.
m_{legs}	920 gr.	l_2	400 mm.	$lfoot_{C13}$	80 mm.
m_{feet}	280 gr.	l_{2K}	200 mm.	$lfoot_{C24-AF}$	120 mm.
M_T	2170 gr.	l_{3K}	200 mm.		

Table 1. Simulation parameters: dimensions and masses

Spring	k	b	q^0 or x^0
Ankle	10	0.4	0
Femur/Knee	8	0.1	0
Knee	750	100	-0.007
Superior Hip	200000	5000	0

Table 2. Simulation parameters: springs

may serve as performance indexes: *(i)* the distance travelled considering the same experimental conditions and *(ii)* the capacity of the robot to walk with a higher tail frequency. Simulation results indicate that the robot with elastic knees is superior to the robot without knees because the former travels larger distances with the same oscillatory frequency (f=0.7 Hz). Moreover, the robot with elastic knees can walk with a higher frequency (f=0.8 Hz), at which the robot without knees falls down. The reason why the robot with knees travels a larger distance is not only because of this higher frequency capacity, but because the robot raises the feet higher in each stride. This is the result of leg spring combination.

As observed in the figures presented in this work, the performance of the two types of robots are very similar, in consumption (Figure 13), in the response of the tail controller (q_0) (Figure 12), in the reaction forces (Figure 8) and in the way the hip angle (q_1) oscillates to pass from the stance phase to the swing phase (Figure 9). Nevertheless, because of the kinematic differences between P_y,s it is difficult to draw definitive conclusions. We conjecture that it is possible for the robot with elastic knees to avoid the lateral sliding mentioned in this paper. This suggests a design of the robot in which the angle q_1 remains constant during the stance phase. Other possibility is a design in which the hip spring of the superior bar allows lateral balancing without sliding, but we have not yet addressed this question.

The way the robot with elastic knees walks is very different from the way the robot without knees walks, in a more compliant way. The limit cycles depicted in Figure 10 show clearly a big difference, but the problem remains in how to compare the two types of robots. One possibility is taking into account their skills. The foot raising height might be an useful criterion if the robot with knees could finally climb stairs. In Gutiérrez et al. (2008) the authors demonstrated that the robot without knees could go up and down different inclination slopes. This was achieved by tuning, in real time, the ankle spring parameter values. Therefore, it produced a modification on the robot equilibrium position, translated in different legs' inclinations. We have proved the same for the robot with knees, but it remains an open question if the robot can climb stairs or turn around. The relaxation of kinematic constraints, we have proposed in this work, points towards this line of research seeking the increase of its manoeuvrability.

6. References

Alexander, R. M. (2005). Walking made simple, *Science Magazine* **308**(5718): 58–59.

Berenguer, F. J. & Monasterio-Huelin, F. (2006). Easy design and construction of a biped walking mechanism with low power consumption, *Proc. of the 9th Int. Conf. Climbing and Walking Robots CLAWAR'06*, Springer-Verlag, Berlin, Germany, pp. 96–103.

Berenguer, F. J. & Monasterio-Huelin, F. (2007a). Stability and smoothness improvements for an underactuated biped with a tail, *Proc. of the 2007 IEEE Symp. on Industrial Electronics*, IEEE Press, Piscataway, NJ, pp. 2083–2088.

Berenguer, F. J. & Monasterio-Huelin, F. (2007b). Trajectory planning using oscillatory chirp functions applied to bipedal locomotion, *Proc. of the 4th Int. Conf. on Informatics in Control, Automation and Robotics*, IEEE Press, Piscataway, NJ, pp. 70–75.

Berenguer, F. J. & Monasterio-Huelin, F. (2008). Zappa, a quasi-passive biped walking robot with a tail. modeling, behavior and kinematic estimation using accelerometers, *IEEE Transactions on Industrial Electronics* **55**(9): 3281–3289.

Boeing, A. & Bräunl, T. (2004). Evolution of locomotion controllers for legged robot, *in* T. et al. (ed.), *Robotic Welding, Intelligence and Automation*, Vol. 299 of *Lecture Notes in Control and Information Sciences (LNCIS)*, Springer-Verlag, Berlin, Germany, pp. 228–240.

Collins, S. H. & Ruina, A. (2005). A bipedal walking robot with efficient and human-like gait, *Proc. of the 2005 IEEE Int. Conf. on Robotics and Automation*, IEEE Press, Piscataway, NJ, pp. 1983–1988.

Fumiya, I., Minekawa, Y., Rummel, J. & Seyfarth, A. (2009). Toward a humanlike biped robot with compliant legs, *Robotics and Automation Systems* **57**(2): 139–144.

Fumiya, I. & Pfeifer, R. (2006). Sensing through body dynamics, *Robotics and Autonomous Systems* **54**(8): 631–640.

Geyer, H. & Seyfarth, A. (2006). Walking and running dynamics explained by compliant legs: Consequences, general insights, and future directions, *Journal of Biomechanics* **39**(1): 361.

Gutiérrez, A., Berenguer, F. J. & Monasterio-Huelin, F. (2008). Evolution of neuro-controllers for trajectory planning applied to a bipedal walking robot with a tail, *in* A. Lazinika (ed.), *New Developments in Robotics, Automation and Control*, I-Tech Education and Publishing, Vienna, Austria.

Ham, R. V., Vanderborght, B., Damme, M. V., Verrelst, B. & D.Lefeber (2007). Maccepa, the mechanically adjustable compliance and controllable equilibrium position actuator: Design and implementation in a biped robot, *Robotics and Autonomous Systems* **55**(10): 761–768.

Hobbelen, D. G. E. & Wisse, M. (2007). Limit cycle walking, *in* M. Hackel (ed.), *Humanoid Robots, Human-like Machines*, I-Tech Education and Publishing, Vienna, Austria.

Hurmuzlu, Y., Génot, F. & Brogliato, B. (2004). Modeling, stability and control of biped robots A general framework, *Automatica* **40**(10): 1647–1664.

Kuo, A. (2007). The six determinants of gait and the inverted pendulum analogy: A dynamic walking perspective, *Human Movement Science* **26**(4): 617–656.

McGeer, T. (1990). Passive dynamic walking, *Int. Journal of Robotics Research* **9**(2): 62–82.

McMahon, T. (1984). *Muscles, Reflexes, and Locomotion*, Princeton Press, Princeton, NJ.

Pfeifer, R. & Bongard, J. C. (2007). *How the Body Shapes the Way We Think: A New View of Intelligence (Bradford Books)*, The MIT Press, Cambridge, MA.

Vukobratovic, M., Borovac, B., Surla, D. & Stokic, D. (1990). *Biped Locomotion: Dynamics, Stability, Control and Application*, Springer-Verlag, Berlin, Germany.

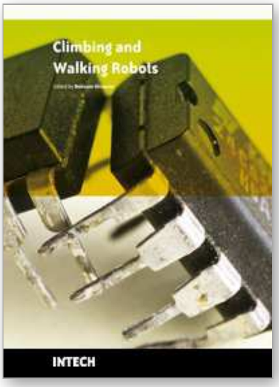

Climbing and Walking Robots
Edited by Behnam Miripour

ISBN 978-953-307-030-8
Hard cover, 508 pages
Publisher InTech
Published online 01, March, 2010
Published in print edition March, 2010

Nowadays robotics is one of the most dynamic fields of scientific researches. The shift of robotics researches from manufacturing to services applications is clear. During the last decades interest in studying climbing and walking robots has been increased. This increasing interest has been in many areas that most important ones of them are: mechanics, electronics, medical engineering, cybernetics, controls, and computers. Today's climbing and walking robots are a combination of manipulative, perceptive, communicative, and cognitive abilities and they are capable of performing many tasks in industrial and non- industrial environments. Surveillance, planetary exploration, emergence rescue operations, reconnaissance, petrochemical applications, construction, entertainment, personal services, intervention in severe environments, transportation, medical and etc are some applications from a very diverse application fields of climbing and walking robots. By great progress in this area of robotics it is anticipated that next generation climbing and walking robots will enhance lives and will change the way the human works, thinks and makes decisions. This book presents the state of the art achievments, recent developments, applications and future challenges of climbing and walking robots. These are presented in 24 chapters by authors throughtot the world The book serves as a reference especially for the researchers who are interested in mobile robots. It also is useful for industrial engineers and graduate students in advanced study.

How to reference

In order to correctly reference this scholarly work, feel free to copy and paste the following:

Felix Monasterio-Huelin, Alvaro Gutierrez and Fernando J. Berenguer (2010). Zappa, a Compliant Quasi-Passive Biped Robot with a Tail and Elastic Knees, Climbing and Walking Robots, Behnam Miripour (Ed.), ISBN: 978-953-307-030-8, InTech, Available from: http://www.intechopen.com/books/climbing-and-walking-robots/zappa-a-compliant-quasi-passive-biped-robot-with-a-tail-and-elastic-knees

INTECH
open science | open minds

InTech Europe
University Campus STeP Ri
Slavka Krautzeka 83/A
51000 Rijeka, Croatia
Phone: +385 (51) 770 447
Fax: +385 (51) 686 166

InTech China
Unit 405, Office Block, Hotel Equatorial Shanghai
No.65, Yan An Road (West), Shanghai, 200040, China
中国上海市延安西路65号上海国际贵都大饭店办公楼405单元
Phone: +86-21-62489820
Fax: +86-21-62489821

© 2010 The Author(s). Licensee IntechOpen. This chapter is distributed under the terms of the Creative Commons Attribution-NonCommercial-ShareAlike-3.0 License, which permits use, distribution and reproduction for non-commercial purposes, provided the original is properly cited and derivative works building on this content are distributed under the same license.